JOURNAL OF MATERIALS SCIENCE **34** (1999) 3335–3340

A calorimetric study of S′ and θ' precipitation in Al_2O_3 particle-reinforced AA2618

I. N. A. OGUOCHA, S. YANNACOPOULOS*
Department of Mechanical Engineering, University of Saskatchewan, 57 Campus Drive, Saskatoon, Canada S7N 5A9

Differential scanning calorimetry (DSC) was used to study the kinetics of S′ and θ' precipitation in AA2618 and its composite containing 15 vol % Al_2O_3 particles. The unreinforced alloy and the composite were fabricated by a proprietary casting method, followed by extrusion. The DSC studies were carried out on as-quenched samples of the test materials. The precipitation of the S′ and θ' phases in both materials was found to be kinetically controlled and obey the modified Avrami-Johnson-Mehl equation. The growth mechanisms for S′ and θ' formation in AA2618 seemed unaffected by the addition of Al_2O_3 particles. The growth parameters obtained for the precipitation of these phases in the matrix alloy and the composite were not significantly different. © *1999 Kluwer Academic Publishers*

1. Introduction

Aluminum alloys with a copper:magnesium weight ratio of 2 : 1 and higher are used for manufacturing a variety of age-hardenable structural alloys. The structural changes that occur during aging of these alloys have been extensively studied [1–7]. According to Silcock [1] and Bagaryatsky [2], the precipitation sequence in the pseudo-binary Al-Al_2CuMg alloy (Al-3wt%Cu-1.5wt%Mg) can be represented as follows:

$$\text{SSS (supersaturated solid solution)} \rightarrow \text{GPB zones} \rightarrow \text{S}'' \rightarrow \text{S}' \rightarrow \text{S} \quad (1)$$

Strengthening of the alloys is associated with the presence of coherent Guinier-Preston-Bagaryatsky (GPB) zones (Cu/Mg clusters) and finely dispersed metastable precipitates: S′(Al_2CuMg) for pseudo-binary Al(α)-Al_2CuMg (S phase) alloys (Cu : Mg $\sim$ 2.2 : 1), and both S′ and θ' (Al_2Cu) for alloys with higher Cu : Mg weight ratios [1]. In the latter alloys, peak hardness is due to co-precipitation of the S′ and θ' phases whereas it is associated with the retention of a greater amount of GPB zones in the presence of S′ in the former alloys. However, both phases have been observed in aluminum alloy 2618 with a copper:magnesium weight ratio of approximately 1.5 : 1 [8].

It is known that GPB zones first precipitate out from the supersaturated solid solution (SSS) during age hardening of Al-Cu-Mg alloys. Their appearance in the first minutes of aging in a wide temperature range (110–240 °C) is mostly based on the interpretation of weak diffraction effects from diffuse X-ray scattering [1, 2]. Silcock reported that the GPB zones are cylindrical, 1–2 nm in diameter and 4 nm long. To date, they have not been observed at this stage of aging by means of conventional electron microscopy techniques, although their presence may be inferred by the pinning of matrix dislocations in the transmission electron microscopy (TEM). Differential scanning calorimetry (DSC) exotherms (range: 50–150 °C) and endotherms (range: 150–280 °C) have been assigned to GPB zone formation and dissolution, respectively [9–15]. However, Ringer *et al.* [5, 6] recently reported that subnanometer Cu/Mg clusters have been observed after a short aging time by means of atom probe field ion microscopy (APFIM) and, consequently, proposed the so-called "cluster hardening" mechanism. This mechanism was reported to be responsible for the initial sharp increase in the hardness and, in their view, these clusters are precursors of GPB zones.

The equilibrium S-Al_2CuMg phase is a face-centered orthorhombic with lattice parameters $a = 0.400$, $b = 0.923$, and $c = 0.714$ nm [16]. The existence of S″ is still in dispute, however, large stresses are considered to be associated with its coherence. Authors in references [1, 3, 7] did not observe it. On the other hand, Alekseev *et al.* [4], Zahra *et al.* [15], Cuisiat *et al.* [17], and Ratchev *et al.* [18] reported evidence of S″ existence. Zahra *et al.* [15] interpreted a hump in the DSC curves (220–250 °C) as a S″ formation peak. Such a peak has been reported by other authors too [9, 12] although it was not directly related to S″ formation. According to Zahra *et al.* [15], during further aging S develops gradually into S′ and S precipitates since no S″ dissolution peak was detected. Ratchev *et al.* [18] reported that S″ formed heterogeneously on dislocation loops and helices. They proposed that its precipitation is the main cause of strengthening during the initial stage

* Author to whom all correspondence should be addressed.

of precipitation hardening (up to 30 min at 180 °C). In addition, they did not observe any link between GPB zones and S″.

Wilson and Partridge [7] have proposed that S″ does not precede S′ and it nucleates heterogeneously on dislocations and dislocation loops, which can relieve partially the misfit between the precipitates and the matrix. The S phase has the same orthorhombic structure as the S′ phase but possesses slightly different lattice parameters ($a = 0.404$, $b = 0.925$, and $c = 0.718$ nm). In view of the fact that the difference in lattice parameters between S′ and S is not appreciable and both phases are indistinguishable in the TEM, some authors have argued that they should not be considered as two separate phases with different notations [3, 6]. Nevertheless, the asymmetric shape of the last exothermic and endothermic DSC peaks in Al-Cu-Mg alloys (in the ranges: 270–350 °C and 350–450 °C) indicates the presence of both S′ and S phases. The non-equilibrium θ' phase has a body-centered tetragonal (bct) structure with lattice parameters $a = b = 0.404$ and $c = 0.580$ nm. The morphology is characterized by a thin, plate-like, ordered pattern. According to Lorimer [19], the precipitation sequence is given as:

$$\text{SSS} \rightarrow \text{GPB zones} \rightarrow \theta' \rightarrow \theta. \qquad (2)$$

Apart from the aforementioned phases, there are indications in the literature that other precipitate phases are present in Al-Cu-Mg alloys. Jin *et al.* [20] and Oguocha *et al.* [8] have reported the existence of X precipitates in AA2124 and AA2618, respectively. Jin *et al.* [20] reported that although both the S and X phases are orthorhombic, their lattice parameters and atomic compositions are different. The lattice parameters of the X phase are: $a = 0.492$ nm, $b = 0.852$ nm, and $c = 0.701$ nm with *Cmmm* space group. Also, their orientation relationships with the matrix are different. It is not clear what influence the X phase has on the overall precipitation kinetics of the Al-Cu-Mg alloys. However, it is believed that its presence is due to differences in matrix composition.

Calorimetric methods have been used to study the kinetics of isothermal and non-isothermal phase transformations in aluminum alloys and metal matrix composites (MMCs) based on aluminum alloys [9–15, 21–26]. Differential scanning calorimetry (DSC) is an attractive and powerful technique for both quantitative and qualitative study of reaction kinetics in materials. With respect to metal matrix composites, it is a very useful evaluation tool for developing new thermal and thermomechanical procedures. It allows several temperature, time, and deformation combinations to be analyzed relatively quickly and the data interpretation is rather unambiguous.

Compared to other techniques for evaluating precipitation kinetics in MMCs (e.g., conventional microhardness and resistivity measurements) where the reinforcing phase renders the material insensitive to detection of microstructural changes [14], DSC is very sensitive to microstructural changes. In a previous DSC study of aluminum alloy 2618 and its composite containing 15 vol % alumina particles [10], the S′ and θ' formation reactions were found to occur in overlapping temperature intervals. As such, any attempt to determine the kinetic parameters for these reactions would require a special technique to deconvolute the unresolved reaction peaks. In the present study, which is a continuation of the previous work, a DSC investigation was undertaken to determine the kinetic parameters for S′ and θ' formation in AA2618 and, also, to investigate the influence of alumina particle addition on the kinetics of these reactions. To make this possible, an approximate deconvolution technique was used to resolve the reaction peaks. The kinetic parameters obtained were compared with published kinetic data for S′ and θ' formation.

2. Materials and Experimental

2.1. Materials

The materials used in this study are aluminum alloy 2618 (Al-Cu-Mg-Fe-Ni) and a 2618 alloy containing 15 vol % alumina particles. The alumina particles are irregularly shaped, with a nominal particle size of 2–20 μm. Both materials were fabricated by Duralcan Inc., San Diego, CA, via a proprietary ingot metallurgy method, followed by extrusion. The compositions of both materials are shown in Table I. The composites are not presently produced commercially; however, the kinetics of precipitation presented in this paper should generally apply to other 2618 Al-based MMCs.

2.2. Procedure

Small slices were cut from the extrudates from which discs (approximately 5 mm diameter, 1–1.2 mm thick) were prepared. The discs were solution heat treated at 530 °C for 2 h and water quenched to laboratory water temperature. DSC tests were conducted on each material in the as-quenched condition using a Mettler TA 4000 thermal analyzer (TA) equipped with a DSC 20 cell. A range of heating rates (from 5 to 30 °C/min) was used. At least two samples of each material were used for each heating rate and the results obtained were found to be reproducible. The DSC scans were initiated at 30 °C and completed at 520 °C. Other details about the experiment have been given elsewhere [10, 12].

3. Results and discussion

The DSC peaks analyzed in this study were assumed to be due to the formation of the three metastable phases mentioned previously (i.e., S′, X′, and θ'). However, in general, the analyses were carried out as if the peaks were due to S-(Al_2CuMg) and Al_2Cu precipitation

TABLE I Composition of test materials

	Element (wt %)[a]								
Material	Si	Fe	Cu	Mn	Mg	Cr	Ni	Zn	Ti
2618 Al	0.18	1.19	2.34	—	1.59	—	1.05	—	0.07
2618 + 15	0.18	1.09	2.11	0.01	1.53	0.004	1.04	0.02	0.07

[a]Balance = Al. 2618 + 15 = 15 vol % Al_2O_{3p}/2618 composite.

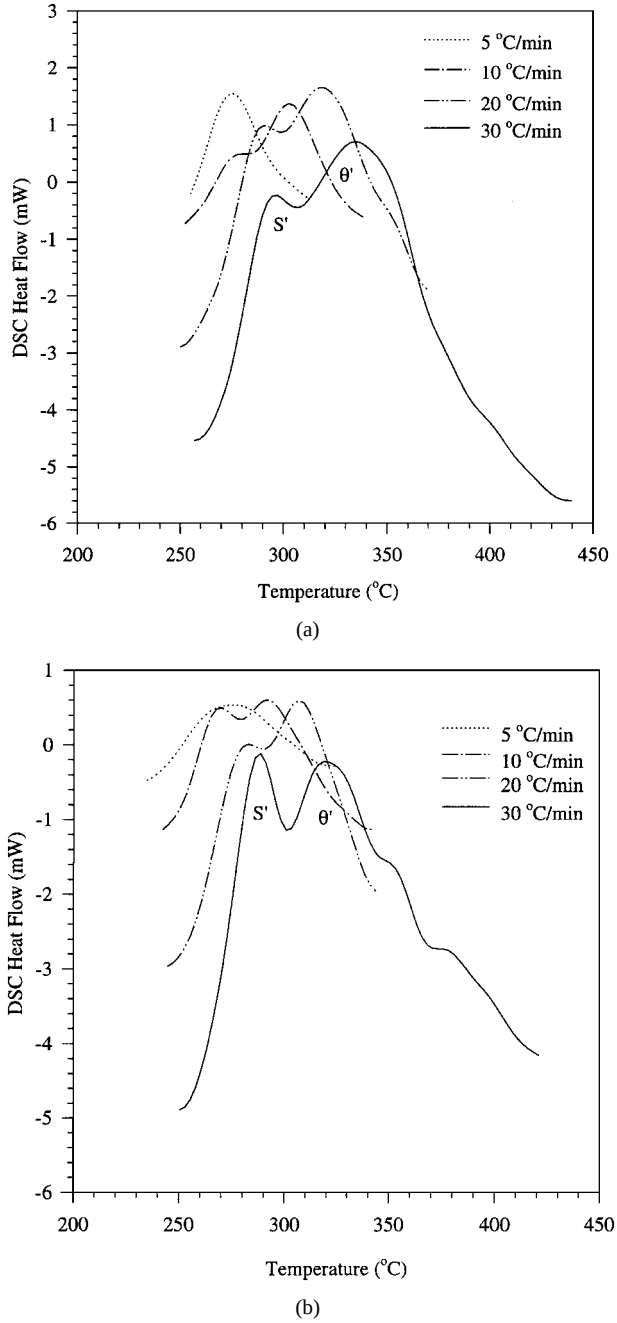

Figure 1 (a) DSC thermograms of as-quenched AA2618 at various heating rates. (b) DSC thermograms of as-quenched 2618 + 15 composite at various heating rates.

reactions only. The DSC signatures shown in Fig. 1a and b are doublet exotherms which represent the formation of the metastable phases in the unreinforced 2618 alloy and the 2618 + 15 composite at different heating rates, respectively. The curves consist of similar heat effects and, as such, the addition of Al_2O_3 particles to 2618 aluminum did not alter its precipitation sequence. Previous DSC studies of Al-Mg-Cu with Cu : Mg weight ratio of 2.1 : 1 showed only a single exothermic peak within this temperature range which the authors [9, 11] attributed to precipitation of the S′ (Al_2CuMg) phase. In 2618 aluminum the Cu : Mg weight ratio is less than 2.2. Therefore, as explained in reference [10], S′ may not be the only phase precipitating in the temperature range.

The literature is not definitive regarding the precise temperatures at which S′ and θ' formation reactions are maximum during DSC scans because the peak reaction temperatures of these phases vary with heating rate, previous thermal history, and material composition. Therefore, two postulations can be made regarding the doublet exotherms: (i) the first peak is due to the simultaneous precipitation of S′ and θ' whereas the second peak is due to their simultaneous growth; (ii) the first peak is due to the formation of S′ phase whereas the second peak is due to the formation of θ' phase. The results obtained in reference [23] for as-quenched ingot metallurgy (IM) aluminum alloys scanned at 10 °C/min show that the θ' formation reaction peaked at 279 °C in AA 2219 whereas the S′ formation reaction peaked at 268 °C in AA2124. Dutta *et al.* [24] reported reaction peaks of 285, 278.7, 277.5 °C for θ' formation in as-quenched AA2014, 10 and 15 vol % Al_2O_3/AA2014 composites, respectively, scanned at 10 °C/min. For AA2124 aged naturally for 30 min prior to a DSC scan at 10 °C/min, it was reported that the S′ formation reaction peaked at 264.7 °C. The data obtained for AA2219-T31 aged naturally for six months show that the θ' formation reaction peaked at 250 °C [11]. On the basis of the quoted literature data, postulation (ii) seems to describe the occurrence of the doublet exotherms better than postulation (i).

3.1. Kinetic parameters for S′ and θ' formation

The determination of the kinetic parameters for S′ and θ' formation was based on the modified Avrami-Johnson-Mehl equation [21], which is given as:

$$y = 1 - \exp(-(kt)^n) \tag{3}$$

where y is the fraction of the excess solute transformed in the time t, n is the growth parameter and k is the rate constant. Fig. 2a and b show respectively the y vs. T and (dy/dT) vs. T plots obtained for S′ formation in unreinforced AA2618 at various heating rates. Similar figures were obtained for θ' and S′ and θ' formation in the composite material. It can be readily seen that the curves shift to higher temperatures with increasing heating rate. However, the unresolved peaks introduce some complications to the anticipated continuous and smooth sigmoid behavior.

There is no accurate graphical scheme for resolving the overlapping S′ and θ' formation reaction peaks. In the present study, an approximate deconvolution method was employed. The total area (A_f) under the S′ peak was calculated by doubling the area between the *onset* temperature and the peak reaction temperature while the total area under the θ' peak was calculated by doubling the area under the *endset* temperature and the peak reaction temperature (see Fig. 3). The modified y vs. T and [(dy/dT)] vs. T plots of the S′ phase in the matrix alloy are shown in Fig. 4a and b, respectively. Similar plots were obtained for the S′ phase in the AA2618 + 15 composite and for θ' in both materials.

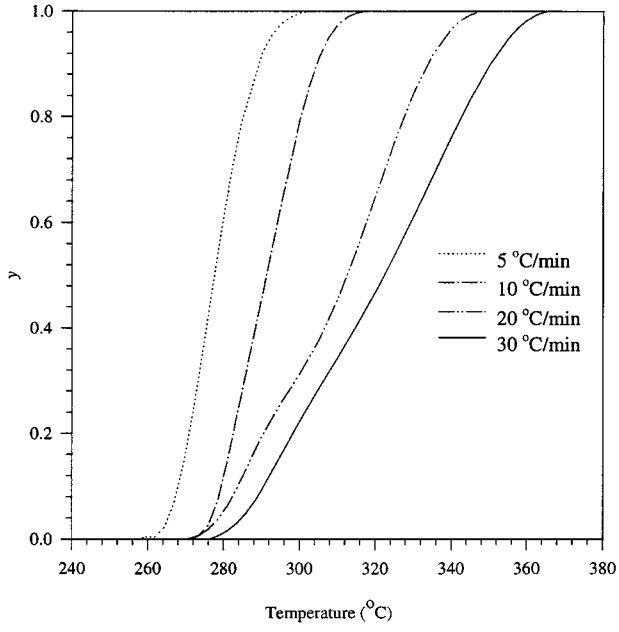

(a)

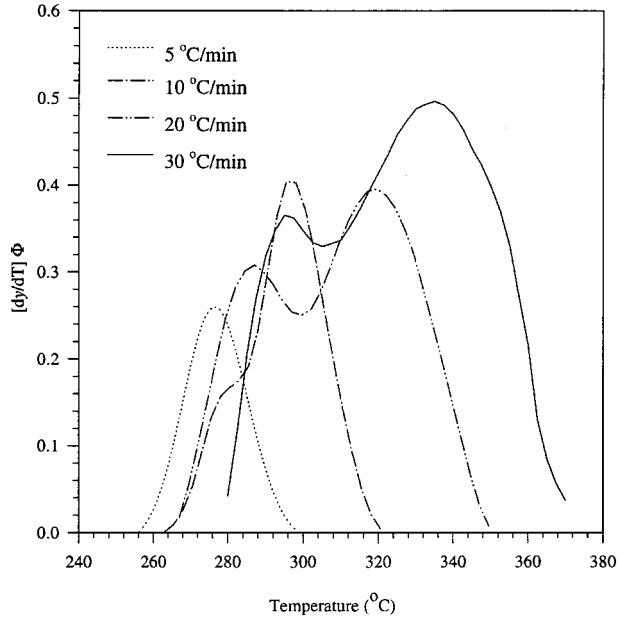

(b)

Figure 2 (a) y vs. temperature curves for S′ and θ' formation in AA2618 at different heating rates. (b) $[(\mathrm{d}y/\mathrm{d}T)\Phi]$ vs. temperature curves for S′ and θ' formation in AA2618 at different heating rates.

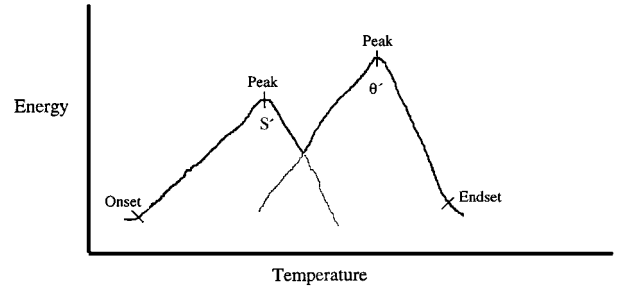

Figure 3 Schematic illustration of A_f determination.

It can be seen from the figures that S′ and θ' precipitation reactions are kinetically controlled in both the unreinforced alloy and the composite material.

The kinetic parameters were calculated using Equations 4 and 5. The latter is the so-called single-heating-

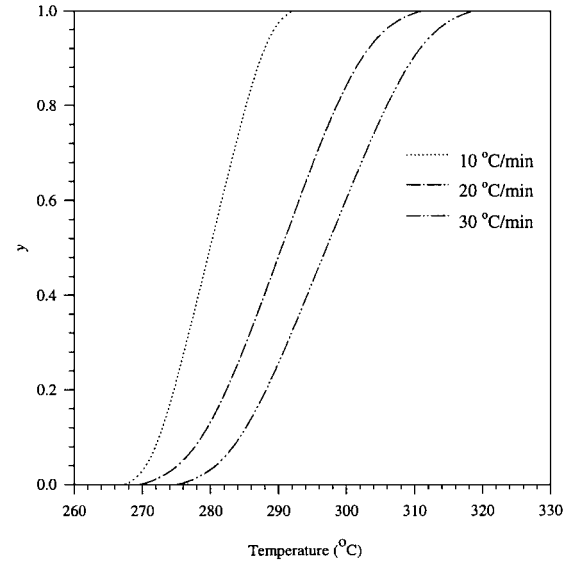

(a)

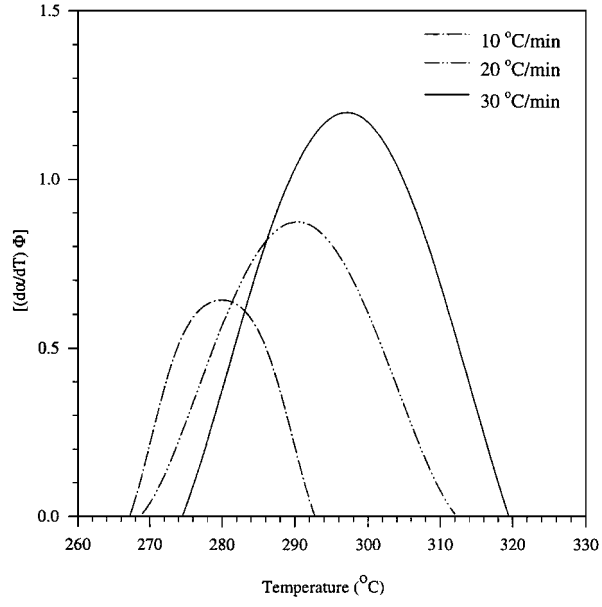

(b)

Figure 4 (a) Modified y vs. temperature curves for S′ formation in AA2618 at different heating rates. (b) Modified $[(\mathrm{d}y/\mathrm{d}T)\Phi]$ vs. temperature curves for S′ formation in AA2618 at different heating rates.

rate relation developed from Equation (3) in references [9, 21]. The results are shown in Table II and Fig. 5a and b for a heating rate $\Phi = 20$ °C/min.

$$f(y) = n(1-y)\left[\ln\left(\frac{1}{1-y}\right)\right]^{(n-1)/n} \tag{4}$$

$$\ln\left[\left(\frac{\mathrm{d}y}{\mathrm{d}T}\right)\left(\frac{\Phi}{f(y)}\right)\right] = \ln k_0 - \frac{E}{R}\left(\frac{1}{T}\right) \tag{5}$$

where E is the effective activation energy describing the overall process whereas k_0, T, and R denote the pre-exponential factor, the absolute temperature, and the gas constant, respectively. The overall activation energy was calculated from $Q = nE$.

Table II shows that $n = 1.54$ for both the unreinforced alloy and the composite for the first exothermic reaction (i.e., S′ formation). This value is close

TABLE II Kinetic parameters for S′ and θ' formation in 2618 and 2618 + 15

	S′ Formation		θ' Formation	
Parameter[a]	2618	2618 + 15	2618	2618 + 15
n	1.54	1.54	1.63	1.52
$k_0(s^{-1})$	2.44×10^{10}	7.66×10^9	1.49×10^7	1.8×10^7
Q (kJ/mol)	170.54	160.17	133.13	123.95
r^2	0.997	0.992	0.988	0.995

[a]Heating rate = 20 °C/min.

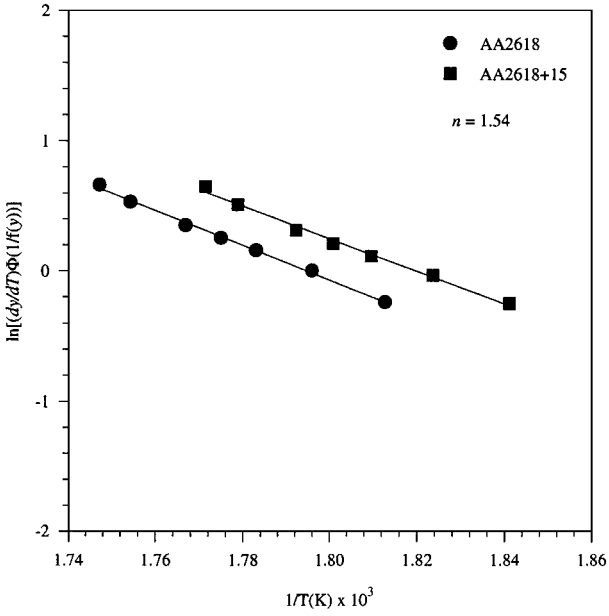

(a)

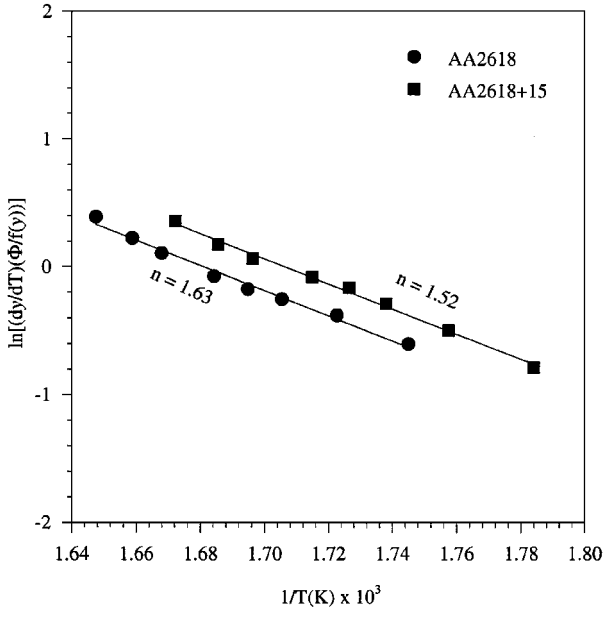

(b)

Figure 5 Arrhenius plots after Equations 4 and 5 for determination of the activation energy for (a) S′ phase formation ($\Phi = 20$ °C/min) and (b) θ' formation ($\Phi = 20$ °C/min).

to the value of growth parameter ($n = 1.56$) obtained by Youdelis and Fang [27] for S′ formation in Be-containing Al-2.5Cu-1.2Mg alloy and is consistent with the observed lathlike morphology for the S phase (one- and two-dimensional growth). Wilson and Partridge [7] reported that S′ precipitates nucleated at dislocation loops and grew as laths on $\{210\}_{Al}$ in a $\langle 100\rangle_{Al}$ direction. The implication of the present result is that the growth mechanism for the S′ phase is not affected by the addition of alumina particles.

The activation energy for the S′ phase formation E (obtained for each material from the slopes of the Arrhenius plots in Fig. 5a and b) is outside the range of values reported by previous workers. Jena *et al.* [9] obtained $Q = 129.9$ kJ/mol for Al-1.53wt%Cu-0.79wt%Mg alloy, Luo *et al.* [21] determined $Q = 132.6 \pm 3.4$ kJ/mol for S′ formation in Al-Li-Cu-Mg alloy, and Youdelis and Fang [27] reported $Q = 109.6 \pm 12.4$ kJ/mol. The discrepancy between the present results and the quoted data may be attributed to differences in material composition, mass transfer resistance, and matrix environment. However, the values of activation energy for S′ formation obtained in this study are within the range of values reported in reference [11] ($Q = 147$ kJ/mol) for PM 2214 aluminum alloy and by Martinod *et al.* [28] ($Q = 158$ kJ/mol).

The kinetics of θ' migration in Al-Cu has been the subject of various studies. In a detailed theoretical and experimental investigation of the structure and migration kinetics of θ' boundaries in Al-4Cu alloy, Aaronson and Laird [29] proposed a ledge mechanism for the thickening of the coherent θ' plates. Although the ledges spread laterally at volume-diffusion-controlled rates, the rate of thickening was found to be interface-controlled and less than that allowed by volume diffusion control. The plates lengthen by jogs on the plate edges, with copper atoms supplied to the jog by pipe diffusion along misfit dislocations. The dislocations provide diffusion short circuits so that the lengthening rate for the plates is faster than allowed by volume diffusion control.

Aaronson and Laird applied several migration models to interpret the experimental results and obtained activation energy ranges for thickening (76.6–115.5 kJ) and lengthening (79.5–98.6 kJ). Merle *et al.* [30] used hardness measurements and TEM to study the growth of θ' and proposed an Avrami type of equation, with an activation energy of 106 kJ to describe the growth kinetics. Chen and Doherty [31] have proposed that θ' thickening can also be described as a volume diffusion process. Papazian [13] used the DSC technique to study θ' formation in 2219 and 7075 aluminum alloys. He reported that the overall process can be described by the Avrami equation (with $n = 1$–1.2) and concluded that the reaction is diffusion controlled. More recently, Karov and Youdelis [32] studied growth kinetics of θ' and θ phases in Al-3Cu alloy. The activation energy for θ' precipitation was determined as $Q = 85.3 \pm 10.9$ kJ/mol. Also, Starink and Mourik [33] reported a Q value of 106.5 ± 9.7 kJ/mol for θ' precipitation in Al-1.66 at % Cu alloy. From Table II, the value of the activation energy obtained for unreinforced AA2618 ($Q = 133.08$ kJ/mol) is outside these activation energy ranges. However, it is within the range of the activation energy for the lattice diffusion of Cu in Al ($Q = 130.6 \pm 6.3$ kJ/mol) reported by Murphy [34]. Thomas and King [11] have summarized the data for elemental diffusion in pure aluminum and simple binary aluminum alloys.

For the θ' phase precipitation, $n = 1.63$ for the unreinforced alloy. This compares fairly well with $n = 1.52$ obtained for the composite material. This is an indication that the growth mechanism for θ' precipitates is unaffected by the presence of alumina particles. The growth parameter obtained for each material is outside the range reported by Papazian [13], but it is close to $n = 1.68$ obtained in reference [32]. On the basis of the growth models proposed by Ham [35], the values of $n = 1.52, 1.63$ are indicative of a disc-like growth which is intermediate between constant plate thickness ($n = 2$) and constant eccentricity ($n = 2/3$, oblate spheroid).

The activation energy for θ' formation obtained for the 2618 + 15 composite ($Q = 123.95$ kJ/mol) lies somewhere between the values for bulk diffusion and grain boundary diffusion of Cu and Mg in aluminum (see Ref. [11]). It is also lower than that of the unreinforced alloy, suggesting that diffusion of the θ' phase is easier in the MMC than in the unreinforced alloy. There are a few published data in this area with which to compare the current results. Dutta *et al.* [24], working on 2014 matrix composites, found a similar trend as in the present work. The values of activation energy they obtained were 82.031, 73.455, and 72.589 kJ/mol for θ' precipitation in unreinforced AA2014, 10 and 15 vol % alumina/AA2014 composites, respectively. Nieh and Karlak [36], working on 6*xxx* matrix MMCs, also found that the activation energy for diffusion was approximately 37% lower in the MMC than in the unreinforced alloy. It was attributed to the enhanced diffusion of solutes along dislocations to growing transition precipitates. This may be the case in the current MMC. Additional diffusion along the Al_2O_{3p}-matrix interfaces may also be a contributing factor. The composite has a larger grain boundary area than the unreinforced alloy due to the smaller sub-grain size. This may contribute to enhanced solute diffusion in the composite matrix.

4. Conclusions

1. The precipitation of metastable S′ and θ' phases are kinetically controlled in both unreinforced AA2618 and its composite. Also, the precipitation sequence of both phases in AA2618 is unaffected by the addition of alumina particles.

2. The formation of S′ and θ' in AA2618 and its 15-vol % alumina-particle reinforced composite obeys the Avrami-Johnson-Mehl equation. The growth parameters for the formation of the S′ and θ' phases are practically the same for both the monolithic alloy and the composite. $n = 1.54$ for S′ formation in both materials whereas, for θ' precipitation, $n = 1.63$ and 1.52 for the monolithic alloy and the composite, respectively. Hence, the addition of Al_2O_3 particles does not seem to alter the growth mechanisms for the formation of these metastable phases.

3. S′ and θ' formation reactions occur earlier in the composite than in the unreinforced alloy.

Acknowledgements

The authors would like to thank Duralcan Aluminum Company, San Diego, CA (USA), for the test materials. Financial assistance from the Natural Sciences and Engineering Research Council of Canada (NSERC) in the form of a research grant to S. Yannacopoulos is hereby acknowledged.

References

1. J. M. SILCOCK, *J. Inst. Metals* **89** (1960-61) 203.
2. Y. A. BAGARYATSKY, *Dokl. Akad. Nauk S. S. S. R.* **87** (1952) 559.
3. A. K. GUPTA, P. GAUNT and M. S. CHATURVEDI, *Phil. Mag.* **55**(3) (1987) 375.
4. A. A. ALEKSEEV, V. N. ANAN'EV, L. B. BER and E. YA. KAPUTKIN, *The Phys. Metals Metallo.* **75**(3) (1993) 279.
5. S. RINGER, K. HONO, T. SAKURAI and I. J. POLMEAR, *Scripta Mater.* **36** (1997) 517.
6. S. RINGER, T. SAKURAI and I. J. POLMEAR, *Acta Mater.* **45** (1997) 3731.
7. R. WILSON and P. G. PARTRIDGE, *Acta. Metall.* **13** (1965) 1321.
8. I. N. A. OGUOCHA, YAN JIN and S. YANNACOPOULOS, *Mater. Sci. Technol.* **13**(3) (1997) 173.
9. A. K. JENA, A. K. GUPTA and M. C. CHATURVEDI, *Acta Metall.* **37**(3) (1989) 885.
10. I. N. A. OGUOCHA and S. YANNACOPOULOS, *Mater. Sci. Eng.* **A231** (1997) 25–33.
11. M. P. THOMAS and J. E. KING, *J. Mater. Sci.* **29** (1994) 5272.
12. I. N. A. OGUOCHA and S. YANNACOPOULOS, *ibid.* **3** (1996) 3145.
13. J. M. PAPAZIAN, *Metall. Trans A.* **13A** (1982) 761.
14. J. L. PETTY-GALIS and R. D. GOOLSBY, *J. Mater. Sci.* **24** (1989) 1439.
15. A. M. ZAHRA, C. Y. ZAHRA, W. LACOM and K. SPIRADEK, in Proc. Int. Conf. on Light Metals, Amsterdam, 20–22 June 1990, edited by T. Khan and G. Effenberg, 1990, p. 633.
16. H. PERLITZ and A. WESTGREN, *Arkiv för Kemi, Miner. Geol.* **12B**(13) (1943).
17. F. CUISIAT, P. DUVAL and R. GRAF, *Scripta Metall.* **18** (1984) 1051.
18. P. RATCHEV, B. VERLINDEN, P. DE SMET and P. VAN HOUTTE, *Acta Mater.* **46**(10) (1998) 3523.
19. G. W. LORIMER, in "Precipitation Processes in Solids," edited by K. C. Russell and H. I. Aaronson (TMS-AIME, Warrendale, PA, 1978) p. 87.
20. Y. JIN, C. LI and M. YAN, *J. Mater. Sci.* **26** (1991) 3244.
21. A. K. GUPTA, A. K. JENA and M. C. CHATURVEDI, *Scripta Metall.* **22** (1988) 369.
22. A. LUO, D. J. LLOYD, A. GUPTA and W. V. YOUDELIS, *Acta Metall. Mater.* **41**(3) (1993) 769.
23. K. K. CHAWLA, A. H. ESMAEILI, A. K. DATYE and A. K. VASADEVAN, *Scripta Metall.* **25** (1991) 1315.
24. J. M. PAPAZIAN, *Metall. Trans. A* **19** (1998) 2945.
25. I. DUTTA, C. P. HARPER and G. DUTTA, *Metall. Mater. Trans. A* **125** (994) 1591.
26. JUN-SHAN LIN, PENG-XING LI and REN-JIE WU, *Scripta Metall. Mater.* **28** (1993) 281.
27. W. V. YOUDELIS and W. FANG, *Mater. Sci. Technol.* **10** (1994) 917.
28. H. MARTINOD, C. RENON and J. CALVET, *Rev. Met.* **63** (1966) 815.
29. H. I. AARONSON and C. LAIRD, *Trans. AIME* **242** (1968) 1437.
30. P. MERLE, F. FOUQUET and J. MERLIN, *Scripta Metall.* **15** (1981) 373.
31. Y. H. CHEN and R. D. DOHERTY, *ibid.* **11** (1977) 725.
32. J. KAROV and W. V. YOUDELIS, *Mater. Sci. Technol.* **2** (1986) 1183.
33. M. J. STARINK and P. VAN MOURIK, *Mater. Sci. Eng.* **A156** (1998) 183.
34. J. B. MURPHY, *Acta Metall.* **9** (1961) 563.
35. F. S. HAM, *J. Appl. Phys.* **30** (1959) 1518.
36. T. G. NIEH and R. F. KARLAK, *Scripta Metall.* **18** (1984) 25.

Received 3 November
and accepted 23 November 1998